Analysis of human brain tissue derived from DBS surgery

Salla M. Kangas*[1,2], Jaakko Teppo[3,4], Maija J. Lahtinen[5,6], Anu Suoranta[7], Bishwa Ghimire[7], Pirkko Mattila[7], Johanna Uusimaa#[1,8], Markku Varjosalo#[3], Jani Katisko#[5,6], Reetta Hinttala#[1,2]

*Corresponding author salla.kangas@oulu.fi

#Shared last author

Affiliations

1 PEDEGO Research Unit, University of Oulu, Oulu, Finland; Medical Research Center, Oulu University Hospital, University of Oulu, Oulu, Finland

2 Biocenter Oulu, University of Oulu, Oulu, Finland

3 Institute of Biotechnology, HiLIFE Helsinki Institute of Life Science, University of Helsinki, Helsinki, Finland

4 Drug Research Program, Faculty of Pharmacy, University of Helsinki, Helsinki, Finland

5 Neurosurgery, Research Unit of Clinical Neuroscience, Oulu University Hospital and University of Oulu, Medical Research Center, Oulu University Hospital, University of Oulu; Oulu, Finland

6 Oulu Research Group of Advanced Surgical Technologies and Physics (ORGASTP), Research Unit of Clinical Neuroscience, Oulu University Hospital and University of Oulu; Medical Research Center, Oulu University Hospital, University of Oulu, Oulu, Finland

7 Institute for Molecular Medicine Finland (FIMM), HiLIFE Helsinki Institute of Life Science, University of Helsinki, Helsinki, Finland

8 Clinic for Children and Adolescents, Division of Pediatric Neurology, Oulu University Hospital, Oulu, Finland

Abstract

The implantation of deep brain stimulation (DBS) electrodes into the human brain is a neurosurgical treatment for, e.g., movement disorders. We describe a novel approach to collecting brain tissue from DBS surgery-guiding instruments for liquid chromatography-mass spectrometry and RNA sequencing analyses. Proteomics and transcriptomics showed that the approach is useful for obtaining disease-specific expression data. A comparison between our improved and the previous approaches and related datasets was performed.

Main

Published proteomics and transcriptomics datasets for different human brain areas are most often based on postmortem material because brain biopsies from living patients are hardly achievable. Neurodegenerative diseases, especially Alzheimer's and Parkinson's, are widely studied using postmortem brain tissue in the search for disease biomarkers and an understanding of the molecular basis of the disease[1,2,3,4,5]. When using postmortem samples, the integrity of brain tissue is compromised due to the delay in collecting the samples, which may bias the results. Some proteins are more prone to degradation than others, and the observed results may depend on postmortem intervals[5,6]. Likewise, RNA is rapidly degraded[7,8], and fresh human brain transcriptome differs from postmortem transcriptome essentially[9]. In their study, Dachet *et al.* showed that, during the postmortem interval, within few hours, neuronal gene expression, especially in the case of brain activity-dependent genes, declines rapidly, while astroglial and microglial gene expression increase reciprocally[9]. In turn, the majority of the housekeeping genes, which are frequently used for normalisation in the comparison of expression levels, are very stable. Also, reduced diversity in the complexity of differentially spliced transcripts in the case of the ultra-complex splicing pattern of RBFOX1 was demonstrated[9]. Therefore, access to fresh brain tissue is critical in obtaining accurate information about brain-specific transcripts and the transcriptome *in vivo*. Using fresh material that is processed within a known time window reduces the technical variation caused by postmortem changes. Biopsies from brain tumors, such as gliomas, are one source of fresh brain-derived tissue that has been utilised quite widely in various omics approaches during past years[10,11], even though they represent the neoplastic phenotype, which does not correspond to normal brain tissue. Recently, approaches that utilise fresh, non-tumorous brain-derived samples from patients treated for various brain-affecting conditions have emerged. For example, brain biopsy samples were collected from patients suffering traumatic brain injury in conjunction with the insertion of an intracranial pressure-monitoring device during corticotomy[12]. Here, our aim was to assess whether the surgical, non-permanent instruments used in the standard DBS implantation procedure contain

enough hemisphere-specific brain-derived material from individual patients for molecular biology analyses, such as RNA sequencing (RNAseq) and liquid chromatography-mass spectrometry (LC-MS), without any sample pooling (Figure 1A).

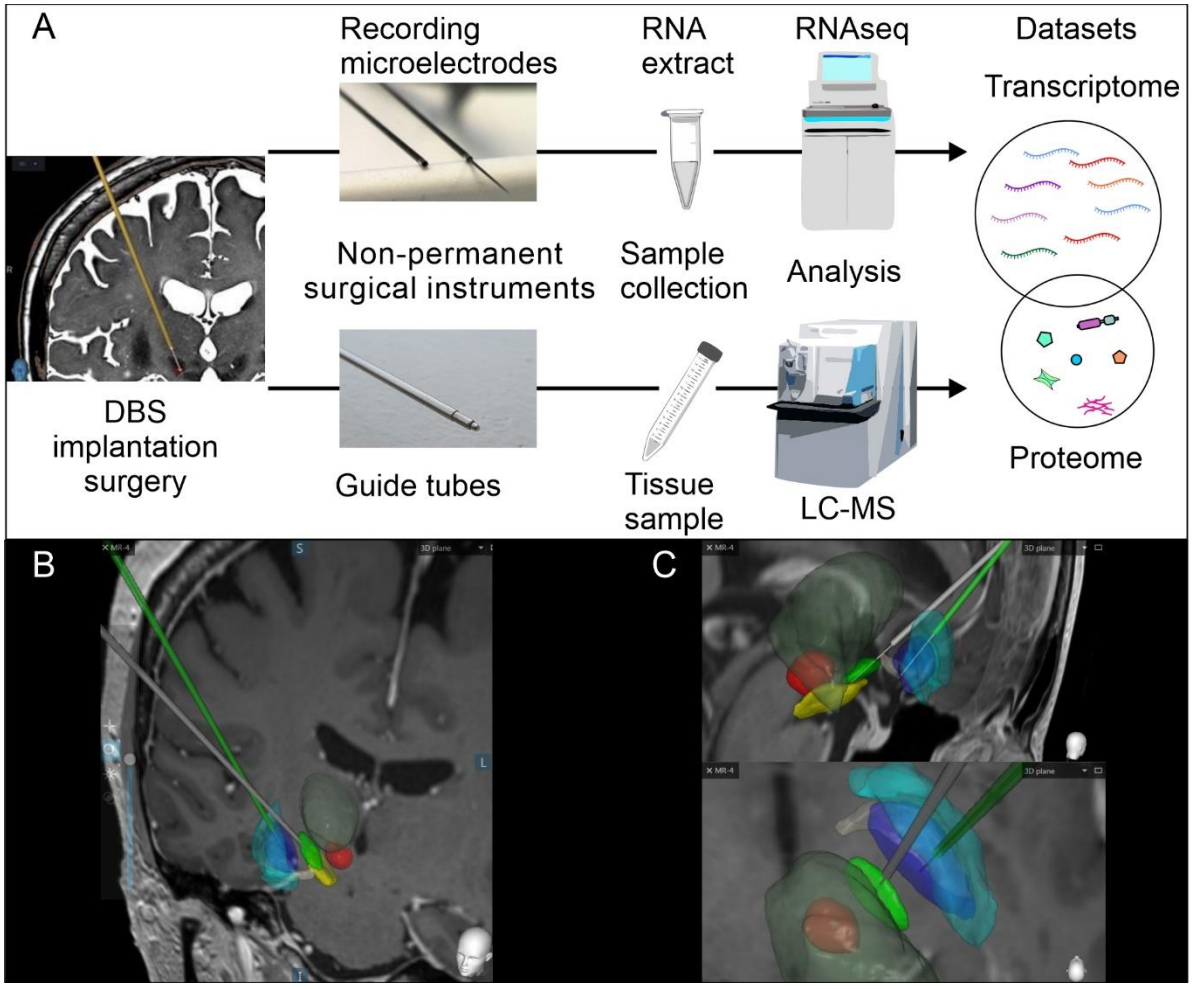

Figure 1. Workflow to collect fresh brain material during DBS surgery for treatment of patients with movement disorders. A) DBS leads were implanted into patients to treat movement disorders in neurosurgical operation at Operative Care Unit, Oulu University Hospital, and the samples were collected from the guide tubes from both hemispheres of 14 patients for LC-MS analysis and the recording microelectrodes of four patients for RNAseq analysis during the standard DBS implantation procedure. The tissue samples for LC-MS were collected from the guide tubes that protruded through the brain tissue to reach the target area and therefore contained tissue material from different brain regions. The RNA samples for sequencing were collected from the recording microelectrodes targeted to the subthalamic nucleus (STN) and globus pallidus interna (GPi). B) The image shows how the guide tubes (grey and green thick lines) passed through brain tissue and the most distal end was 10 mm from the planned target. C) In contrast, the microelectrodes (thin grey lines) travel inside the guide tube, and they touched brain tissue only in the STN (green area) and GPi (blue area). To help with anatomical orientation, the other brain structures are the thalamus (dark transparent green), substantia nigra (yellow), red nucleus (red), ansa lenticularis (dark white) and globus pallidus externa (transparent turqoise).

Deep brain stimulation (DBS) is a neurosurgical treatment for advanced and medically refractory movement disorders, such as Parkinson's disease, essential tremor and dystonia. In addition, pain, epilepsy and psychiatric disorders are increasingly treated with DBS[13]. During DBS operation, intracranial electrodes are targeted into specific locations in the deep brain structures bilaterally. The intracranial leads are connected to an external impulse generator through extension leads. The DBS device stimulates deep brain structures with a low-level electrical current that alleviates patients' symptoms in a reversible manner. The location of the intracranial electrodes is most commonly in the deep basal nuclei, and the most common trajectory to the target area is through the posterior parts of the frontal lobes (Figure 1B-C). The patient-specific targeting of intracranial electrodes is planned on brain magnetic resonance images (MRI) and adjusted with intraoperative clinical testing and microelectrode registration (MER) during neurosurgical operation if patient is awake. The normal surgical procedure for DBS implantation followed by Operative Care Unit at the Oulu University Hospital is described in more detail in the previous publication[14]. Here, we demonstrate the collection of fresh brain tissue samples from single-use surgical instruments, guide tubes and recording microelectrodes, which are needed for the standard DBS electrode implantation into movement disorder patients, and the omics datasets derived from subsequent analyses of the tissue material at the RNA and protein levels. The samples were collected from 17 patients treated with DBS at the Operative Care Unit at Oulu University Hospital for RNA-seq (n=4) and LC-MS (n=14) (Tables 1 and 2, respectively).

Table 1. Info about patients and samples for RNA-seq analysis.

Patient	Sex	Age	Movement disorder	DBS target area	Sample ID	Brain hemisphere	Number of transcripts identified
1	M	8	Dystonia	Gpi	DYT1R_C DYT1L_C	right left	19343 23817
15	M	67	PD	STN	PD12L PD12R	left right	22411 21522
16	F	60	Dystonia	Gpi	DYT3L DYT3R	left right	11861 20440
17	F	61	PD	STN	PD13R PD13L	right left	21880 17311

Table 2. Info about patients and samples for LC-MS analysis.

Patient	Sex	Age	Movement disorder	DBS target area	Sample ID	Brain hemisphere	Visible blood	Total protein (µg)	Number of proteins identified
1	M	6	Dystonia	Gpi	DYT1L_A	left	yes	453.11	181
					DYT1R_A	right	no	4.28	298
2	M	54	Tremor	VIM	TRE1R	right	no	8.51	217
					TRE1L	left	no	NA	190
3	M	67	PD	STN	PD1L	left	no	NA	165
					PD1R1	right	no	14.25	375
					PD1R2	right	no	NA	218
4	F	58	PD	STN	PD2R	right	yes	82.63	199
					PD2L	left	no	6.03	319
5	M	58	PD	STN	PD3L	left	yes	86.80	153
					PD3R	right	yes	148.61	252
6	M	62	PD	STN	PD4L	left	yes	63.82	211
					PD4R	right	yes	93.01	175
7	M	59	PD	STN	PD5R	right	no	2.36	244
					PD5L	left	yes	87.60	262
8	F	67	PD	STN	PD6R	right	no	NA	292
					PD6L	left	yes	20.07	161
9	M	59	PD	STN	PD7L	left	no	3.87	136
					PD7R	right	no	NA	150
10	M	52	PD	STN	PD8R	right	no	NA	193
					PD8L	left	no	NA	67
11	F	63	Dystonia	Gpi	DYT2L	left	no	NA	120
					DYT2R	right	no	NA	200
12	M	59	PD	STN	PD9L	left	no	NA	178
					PD9R	right	yes	9.24	261
13	F	66	PD	STN	PD10L	left	yes	14.79	223
					PD10R	right	no	2.51	211
1	M	7	Dystonia	Gpi	DYT1L_B	left	yes	50.52	163
					DYT1R_B	right	yes	48.88	287
14	F	62	PD	STN	PD11R	right	no	NA	169
					PD11L	left	no	NA	204

Zaccaria *et al.* have previously utilized deep brain stimulation (DBS) surgery to obtain brain-derived material, which they termed "brain tissue imprints" (BTIs), for proteome and transcriptome analysis from Parkinson's disease patients[15]. To our knowledge, this is the only published method that resembles ours; however, there are substantial differences in procedure (Table 3). Zaccaria *et al.* collected 19 samples from twelve patients as follows[15]: After determining the DBS target area via MER, a blunt stylet, as an additional sample collection step, was inserted through the guide tube into the brain for one minute to obtain material for analyses. The material attached to the stylet was then used for proteomics, electron microscopy, immunohistochemistry and immunofluorescence or RNA microarray analysis. In our protocol, no alterations or additional steps were introduced to the

standard DBS procedure; instead, we collected the brain tissue material that had attached to the guide tubes and recording microelectrodes used during the normal surgical procedure. Because our DBS implantation surgery followed standard procedure, we were able to collect samples systematically from the both hemispheres of each patient, whereas the protocol used by Zaccaria *et al.* had technical constraints that allowed sample collection procedure from both hemispheres only occasionally.

Table 3. Comparison of the two approaches to collect and analyze samples obtained during DBS surgical procedure. Our method was compared to the method previously published by Zaccaria *et al.*[15].

	Sample collection procedure described in the current paper	**BTI method[15]**
Sample collection protocol	Method does not require any additional modifications to standard DBS implantation procedure. The brain tissue attached to the guide tubes and microelectrodes were used for sample preparation for proteomics and transcriptomics.	Modification to the standard DBS implantation procedure: A blunt stylet was inserted through the guide tube into the brain tissue during DBS implantation procedure for one minute for obtaining material for analyses.
Sample usage	Both RNA-seq and LC-MS analyses can be carried out from the same individual patients and their separate hemispheres (if patient is awake during the procedure).	Tissue sample was used either for RNA extraction for microarray analysis or pooled from six samples and, after in-gel fractionation, analyzed using Nano-LC-MS/MS.
Transcriptomics	The tissue material for RNA-seq was collected from the recording microelectrode targeted to the specific well-defined area in the deep brain region.	RNA microarray from the tissue sample attached to the blunt stylet was carried out after application of double amplification protocol.
Proteomics	No pooling of samples. Hemisphere-specific MS data was obtained from the tissue collected from the guide tube that has passed through different brain regions to reach the target area.	Six samples from different patients and brain hemispheres were collected from the blunt stylet and pooled for in-gel fractionation and subsequent MS analysis.
Applications	Identification of patient- and/or disease-specific transcripts, proteoforms and post-translational modifications.	BTI samples were used for immunocytochemistry to identify neuronal and glial cell types in the tissue.

In our approach, transcriptomic analysis was focused on the subthalamic nucleus (STN) or globus pallidus interna (GPi) regions, which are specific targets of DBS in treating patients with movement disorders. Samples for RNA-seq were collected separately from both hemispheres of four patients (Supplemental Table S1), of whom two had Parkinson's disease and STN as the target area and two had genetic dystonia and GPi as the target area (Figure 1C). The number of identified genes expressed in the eight samples varied from 11,861 to 23,817 (Figure 2A), of which 32,034 genes were unique across all the samples (Supplemental Data S1). In total, 14,562 genes were identified in all samples from the STN (Figure 2B), and 10,638 genes were identified in all samples from the GPi (Figure 2C). Also, 9,901 genes were commonly detected in all samples from both brain regions.

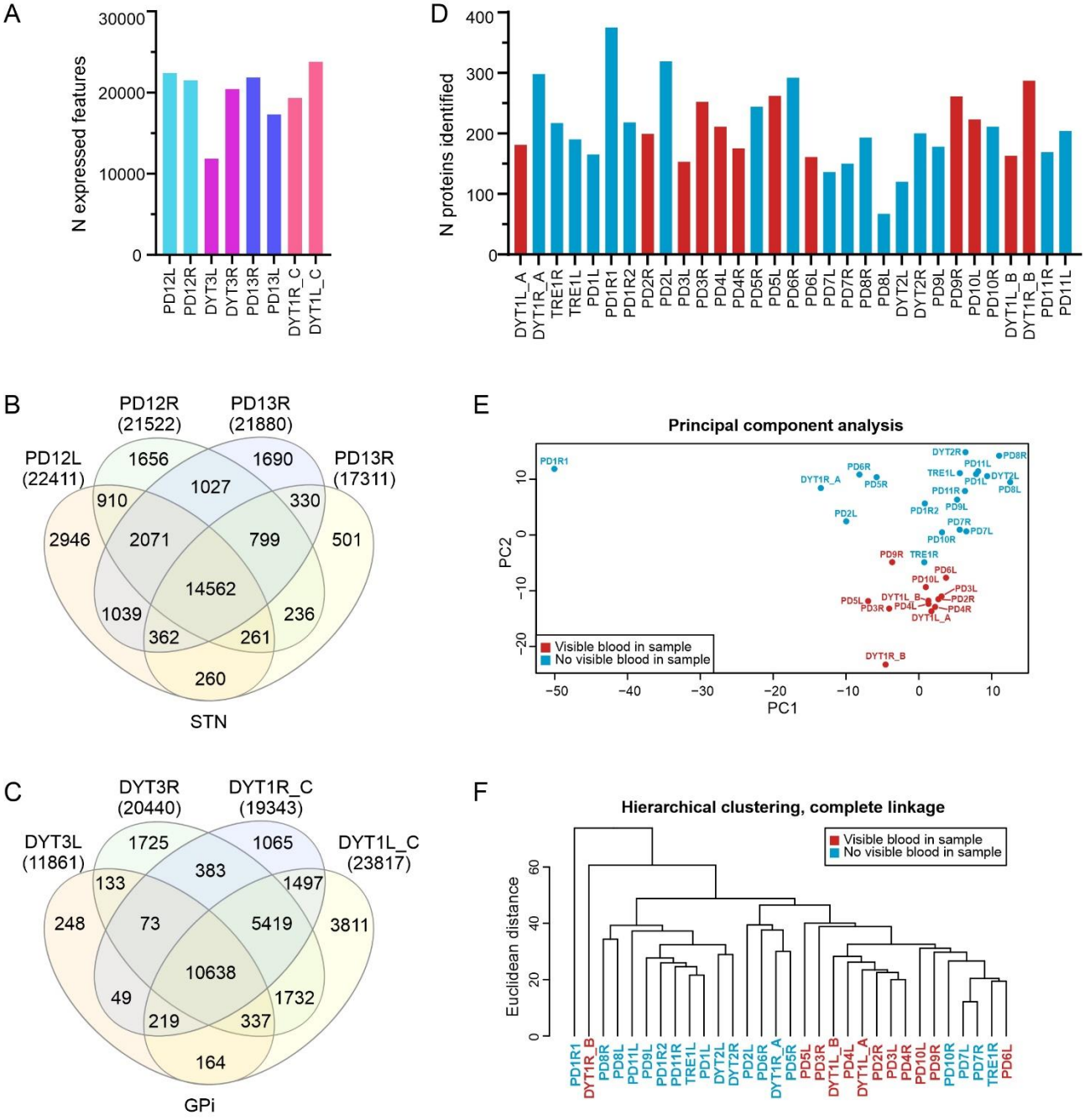

Figure 2. Features of proteomics and transcriptomics datasets obtained from the RNA sequencing and LC-MS analyses of the patient-derived brain tissue. The sample encoding indicates the patients' disorders are as follows: Parkinson's disease (PD, n=13), genetic dystonia (DYT, n=3) and tremor (TRE, n=1). A) The number of expressed genes in each sample. Venn diagrams show the number of common genes identified in the samples from B) the subthalamic nucleus (STN) and C) the globus pallidus interna (GPi) target areas. D) The number of identified proteins in each sample, colored based on whether blood was visible in the sample. No statistical difference in the number of proteins identified was observed (t-test p=0.51). E) Principal component analysis (PCA) plot of the proteomic data and F) hierarchical clustering, colored based on whether blood was visible in the sample, shows that samples with visible blood tend to cluster.

After confirming by immunoblotting that brain-specific proteins were present in the tissue material collected from guide tubes (Supplemental File S1), we proceeded with proteomics analysis. By using LC-MS, we could identify 734 unique proteins from 31 samples from 14 patients (Table 2). Eighteen of these proteins (seven being abundant in blood) were present and quantified in all samples (Supplemental Data S2). Based on visual inspection, the samples contained variable amounts of blood, which did not influence on the overall number of proteins identified in those specific samples (Figure 2D, Supplemental Data S2). However, the clustering of the samples according to the blood observed in them was evident (Figures 2E and 2F). When we analysed the identified protein datasets using DAVID[16,17], we found that the enriched GO terms reflected the brain tissue well, and blood, which was observed in some of the samples, was not over-represented among these terms (Figure 3F, Supplemental Data S2). However, we believe that the removal of blood from the samples prior to the LC-MS analysis will improve the specificity of the assay, if managed with minimal sample loss. When the transcriptomics dataset was mapped to Uniprot identifiers, the overlap between the transcriptomics dataset and proteomics dataset was 686 identifiers, which covers 93,5% of identified proteins.

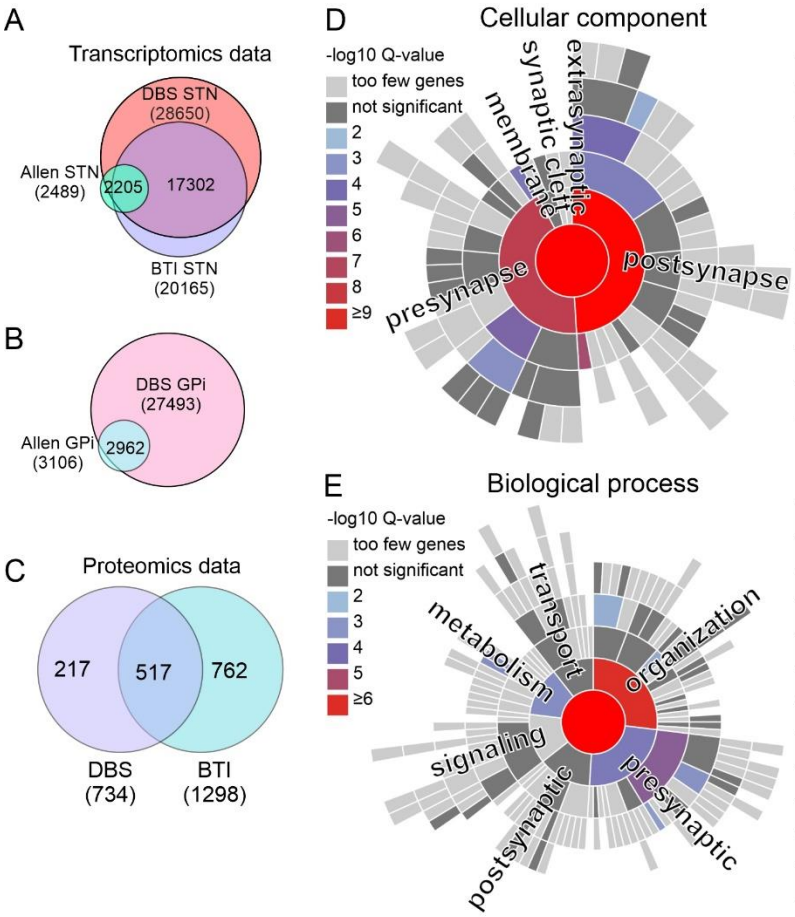

GO term name - hierarchical structure	# genes	FDR corrected p-value
synapse	226	2,8E-21
├─ **postsynapse**	138	4,8E-13
│ ├─ postsynaptic ribosome	29	4,8E-07
│ ├─ postsynaptic specialization	59	3,1E-04
│ │ ├─ postsynaptic density	53	8,9E-05
│ │ │ ├─ postsynaptic density, intracellular component	13	3,9E-03
├─ **presynapse**	103	3,2E-08
│ ├─ synaptic vesicle	32	4,2E-05
│ │ └─ synaptic vesicle membrane	6	8,1E-04
│ ├─ presynaptic ribosome	19	2,2E-04

GO term name - hierarchical structure	# genes	FDR corrected p-value
process in the synapse	156	3,3E-09
├─ **synapse organization**	68	1,0E-06
│ ├─ postsynapse organization	19	3,2E-03
│ │ └─ structural constituent of postsynapse	10	4,5E-03
├─ **metabolism**	26	6,9E-04
│ ├─ protein translation at presynapse	18	6,9E-04
│ └─ protein translation at postsynapse	19	6,9E-04
├─ **process in the presynapse**	52	2,4E-04
│ ├─ synaptic vesicle cycle	44	4,0E-05
│ │ └─ synaptic vesicle endocytosis	17	9,1E-04
│ │ ├─ synaptic vesicle proton loading	9	1,7E-03

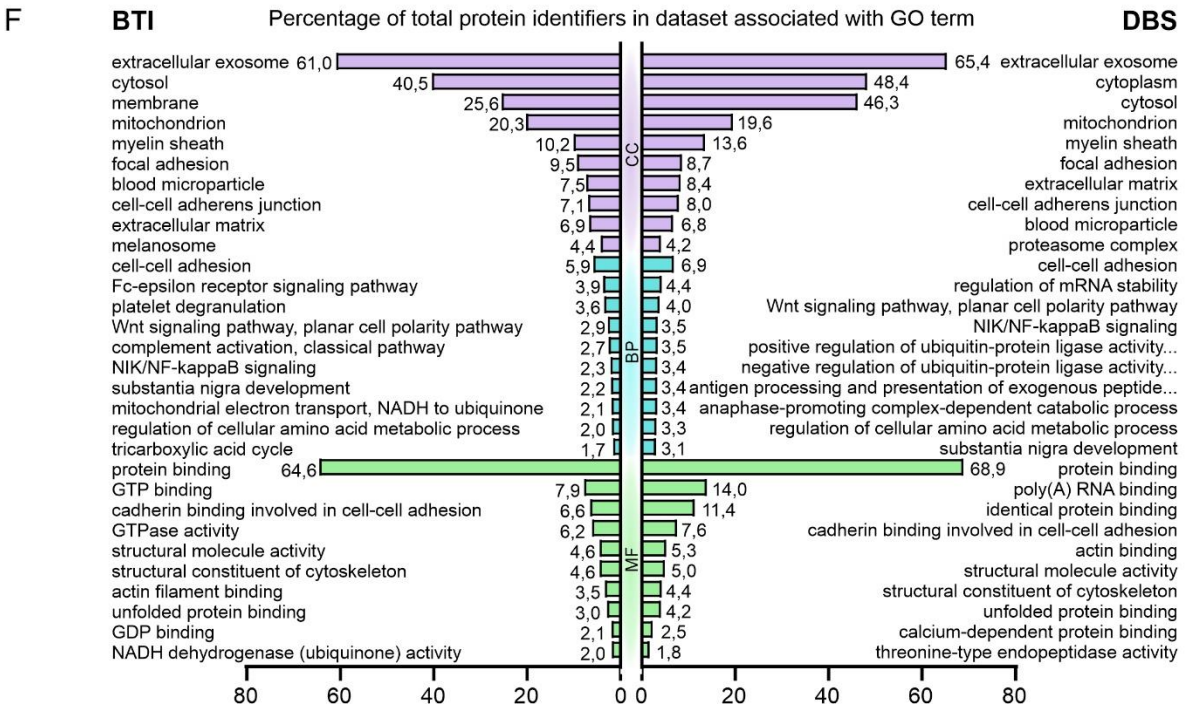

Figure 3. Comparison of the datasets to other published data and Gene Ontology (GO) enrichment analyses. We compared our target region-specific transcriptomics datasets to the anatomically specific expression datasets in Allen Brain Atlas and found substantial overlap in A) STN- and B)

GPi-specific terms. The BTI dataset contained only STN data, and we found that our data had 86% overlap with the BTI dataset. C) We compared our dataset of all unique protein identifiers to the BTI proteomics dataset[15] and found that 517 identifiers out of 734 (70%) were in common with the BTI dataset. We tested the top 20% expressed RNAseq identifiers common to all analysed samples (n=1,980) using the SynGO Knowledge base gene set enrichment tool[19]. D) Ten terms in the cellular component category and E) eleven terms in the bioprocess category were significantly enriched at 1% FDR (testing terms with at least three matching input genes). F) To obtain an overview of the type of proteins identified, GO enrichment analysis using DAVID bioinformatics platform Version 6.8 was performed to the list of all identified proteins across all the samples. We also performed the same analysis to the BTI dataset published previously by Zaccaria *et al.* [15] to compare the outcomes of these two methods. The top 10 most enriched terms in each GO category (Cellular component, CC; Biological process, BP; Molecular function, MF) show that our dataset shares many top terms with the BTI dataset.

The datasets achieved via our method were compared to the BTI approach previously described by Zaccaria *et al.* [15] In their transcriptomics analysis, Zaccaria *et al.* produced three RNA microarray datasets from the STNs of three patients, containing 35,701; 29,842 and 27,350 detected unique microarray probe identifiers. We converted the probe identifiers from the BTI RNA microarray dataset into 20,165 unique Ensembl gene (ENSG) identifiers to allow comparison with our dataset. Ultimately, 17,302 unique identifiers (86%) were common between our STN-specific RNAseq and BTI microarray datasets (Figure 3A). We also compared our STN- and GPi-specific RNAseq datasets to brain region-specific expression datasets representing up-regulated genes in the STN (Figure 3A) and GPi (Figure 3B) (Allen brain atlas[18]) and found that a substantial majority (85% and 95%, respectively) of the upregulated genes were present in our datasets. The BTI protocol for sample acquisition led to the identification of 1,298 unique proteins from the samples using Nano-LC-MS/MS[15]. We compared the list of our identified proteins to the BTI proteomics dataset and found that 70% of the proteins in our dataset are common with the BTI proteomics dataset (Figure 3C).

SynGO is a knowledgebase that focuses on synapse-specific ontologies, and its annotations are based on published, expert-curated evidence[19]. In their study, Koopmans and others show that synaptic genes are exceptionally well conserved and less tolerant of mutations than other genes[19]. They conclude that many SynGO terms are overrepresented for genes that have variants associated with brain disease. By using the SynGO analysis tool, we could identify several terms enriched among the 20% top of expressed genes (Figures 3D and 3E, Supplemental Data S3), and 68% (754/1,112) of SynGO annotated genes were found in our RNAseq dataset, which contained 9,901 genes overlapping all the eight samples. This indicates that the RNAseq data obtained from the tissue attached to the recording microelectrodes during the DBS implantation procedure are a

potentially useful resource in studying brain disorders and the brain-specific transcriptome landscape, such as brain-specific transcript isoforms *in vivo*.

The GO enrichment analysis of the BTI proteomics dataset via DAVID revealed that both datasets have many similar GO term profiles in their top 10 enriched terms (Figure 3F). For their analysis, Zaccaria *et al*. pooled samples from six patients and brain hemispheres for in-gel fractionation and subsequent MS analysis, whereas our data are both patient- and hemisphere-specific[15]. In general, sample pooling increases the number of proteins identified, but it also leads to the loss of information on sample variation, the missed detection of biomarkers and the false identification of others[20]. Molinari *et al.* found that pooled samples are not equivalent to average of biological values and pooling affects statistical analysis[20]. The pooling of the BTI samples[15] for downstream analyses has led to the loss of substantial patient- and hemisphere-specific information, whereas our datasets are patient- and hemisphere-specific.

These results indicate that our improved approach to collecting patient-derived fresh brain tissue from instruments used for DBS implantation surgery is useful in studying brain disorders at the individual hemisphere level. The collection of defined patient cohorts and comparisons of the disease-specific brain proteomes and transcriptomes are a valuable tool for use in identifying disease signatures. Compared to postmortem samples, DBS implantation-derived samples present earlier time points in the disease course and phenotype, which helps in understanding the changes that occur at defined clinical stages during the development of neurological symptoms. One potential caveat regarding this approach is a lack of healthy controls, but a comparison of the molecular signatures between different diseases and stages of disease progression allows the identification of common brain-specific proteoforms and transcripts, as well as novel disease-specific markers, for further studies. As essential improvements to the BTI approach previously described by Zaccaria *et al.* [15], our method does not make any modifications to our standard surgical DBS procedures, and our approach allows collecting samples from the guide tubes from both hemispheres of the patients routinely, without sample pooling for subsequent analyses. If a neurosurgical operation is performed on a conscious patient to perform MER and thus adjust the target region, at the same time, samples for transcriptomics can also be collected from the microelectrodes representing a very defined brain target area. In contrast to this highly region-specific transcriptomics analysis, our proteomics analysis provides data from a cross-section of the brain, containing an expression profile from a mixture of cell types from different brain layers.

The improved approach we describe here can be used to bring novel information about brain tissue-specific transcript variants from specific brain regions, proteoforms and post-translational

modifications, which represents valuable additional knowledge about the brain transcriptome and proteome landscape *in vivo*. Analysis of fresh brain material is important because postmortem changes lead to a rapid loss of transcriptomic diversity in neuronal tissue and glial activation causes the upregulation of gene expression that does not correspond the normal expression landscape of the brain tissue [9]. In the future, as proteomics and transcriptomics techniques become more sensitive and new methods are developed, the approach described here will be a valuable tool with which to access fresh brain-derived material for novel discoveries. By combining the patient-derived proteomics and transcriptomics data with experiments utilising patient-derived cells and disease modelling, this approach advances personalized medicine and studies in the field of neurological diseases.

The RNAseq and LC-MS datasets are described and available via the BioStudies database (https://www.ebi.ac.uk/biostudies/) under accession number BSST667.

Materials and Methods

Ethical permits

The study protocols of the DeepCell project concerning the research on patient samples have been approved by the Ethics Committee of the Northern Ostrobothnia Hospital District (DeepCell, EETTMK:107/2016). All patient-derived samples for research were obtained based on voluntary participation in the study, and written informed consent was obtained from all patients or parents or guardians of such participating in this study under the guidance of a physician. When personal information on a patient is collected, stored, accessed and used, special attention was paid to the protection of the confidentiality of the subject according to the European Directive 95/46/EC.

Patients

Deep brain stimulator (DBS) leads were implanted into patients during neurosurgical operations at the operative care unit, Oulu University Hospital, Finland, between October 2017 and June 2019. The indications for DBS treatment were Parkinson's disease (n=13), genetic dystonia (n=3) and tremor (n=1). Guide tubes and microelectrodes were used during the standard DBS implantation procedure (Figure 1). The samples were collected from the recording microelectrodes collected from four patients (eight samples) for RNA sequencing (RNAseq)(Table 1) and guide tubes from 14 patients (31 samples) for liquid chromatography-mass spectrometry (LC-MS) (Table 2). When extracting the RNA from the recording microelectrodes, the target region was the STN (n(patients)=2, n(samples)=4) and Gpi (n(patients)=2, n(samples)=4). When collecting the tissue

from the guide tubes, intracranial leads were targeted into the subthalamic nucleus (STN, n(patients)=11, n(samples)=23), globus pallidus interna (Gpi, n(patients)=2, n(samples)=6), or ventral intermediate nucleus of the thalamus (VIM, n(patients)=1, n(samples)=2). The LC-MS samples from Patients 4 and 6 (sample codes PD2 and PD4, respectively) were obtained during re-implantation to resume DBS treatment after the previous removal of the DBS leads due to technical failure. Two samples, one from each hemisphere (coded L=left or R=right), were obtained from each patient during the procedure, with one exception. Three guide tubes, of which two (PD1R1 and PD1R2) were from the right hemisphere, were obtained from Patient 3.

From Patient 1, three sets of samples were obtained from three separate surgical procedures. The first samples (DYT1L_A and DYT1R_A) were collected from the guide tubes for LC-MS analysis during the first DBS implantation procedure. The second samples were collected for LC-MS analysis during revision surgery, which was performed due to technical failure. The brain tissue samples were collected from the revised DBS leads. The third samples (DYT3L_A and DYT3R_A) were collected for RNAseq from the recording microelectrodes during the reimplantation of the DBS.

DBS implantation procedure

The surgical procedure for DBS implantation was carried out according to the standard protocol in our institute, as described in detail by Lahtinen *et al.* [14]. The guide tubes (Universal Guide Tube, Elekta, Stockholm, Sweden) and recording microelectrodes (Leadpoint, Alpine Biomed, Skovlunde, Denmark) used during the implantation procedure were collected and used for sample acquisition for proteomics and transcriptomics, respectively.

RNA extraction for RNAseq

After the removal from the brain, the recording microelectrode was taken to a research laboratory on ice, where it was immediately immersed in 700 µl of QIAzol Lysis Reagent (Qiagen) at room temperature and triturated by using lead as a piston. The microelectrode was kept in QIAzol Lysis Reagent for about 10 minutes and triturated once more before discarding the electrode. The sample was briefly vortexed (2–3s) and stored at -80C. RNAseq was performed by the sequencing unit of the Institute for Molecular Medicine Finland FIMM Technology Centre, University of Helsinki.

RNAseq

Total RNA was extracted with a Qiagen miRNeasy micro kit (QIAGEN, Hilden, Germany), according to the kit handbook. The quality and quantity of the extracted RNA samples were analyzed with a 2100 Bioanalyzer using an RNA 6000 Pico Kit (Agilent, Santa Clara, CA, USA). Paired-end cDNA libraries were prepared from 0,2 ng of extracted RNA, with eleven cycles of amplification using a SMART-Seq v4 Ultra Low Input RNA Kit, according to the manufacturer's user manual (Takara Bio USA, Inc. Mountain View, CA, USA). One hundred pg of amplified cDNA was tagmented and indexed for sequencing using a Nextera XT DNA Library Prep Kit (Illumina, San Diego, CA, USA). LabChip GX Touch HT High Sensitivity assay (PerkinElmer, USA) was used for quality measurement and quantification of the purified dual-indexed libraries for equimolar pooling. The sequencing of the pooled samples was performed with an Illumina NovaSeq 6000 System (Illumina, San Diego, CA, USA). The read length for the paired-end run was 2x101 bp, and the target coverage was 15 M reads for each library.

RNAseq data analysis

The RNAseq datasets were analyzed using FIMM-RNAseq data analysis pipeline Version v2.0.1. (Figure 4). The pipeline is implemented in Nextflow[21]. Nextflow allows the portability and scalability of the pipeline and supports major cloud computing and batch processing technologies. More importantly, the pipeline allows the reproducibility of the results by using a version labeled set of software dependencies, a Conda environment. A Conda environment can be created manually, or Nextflow can be instructed to create one during a run-time without an effort. Alternatively, a readily available Docker image containing all software dependencies can be used to run the pipeline in a containerized computing environment, such as Docker and Singularity. Source code and a comprehensive user's manual of the pipeline is available at https://version.helsinki.fi/fimm/fimm-rnaseq

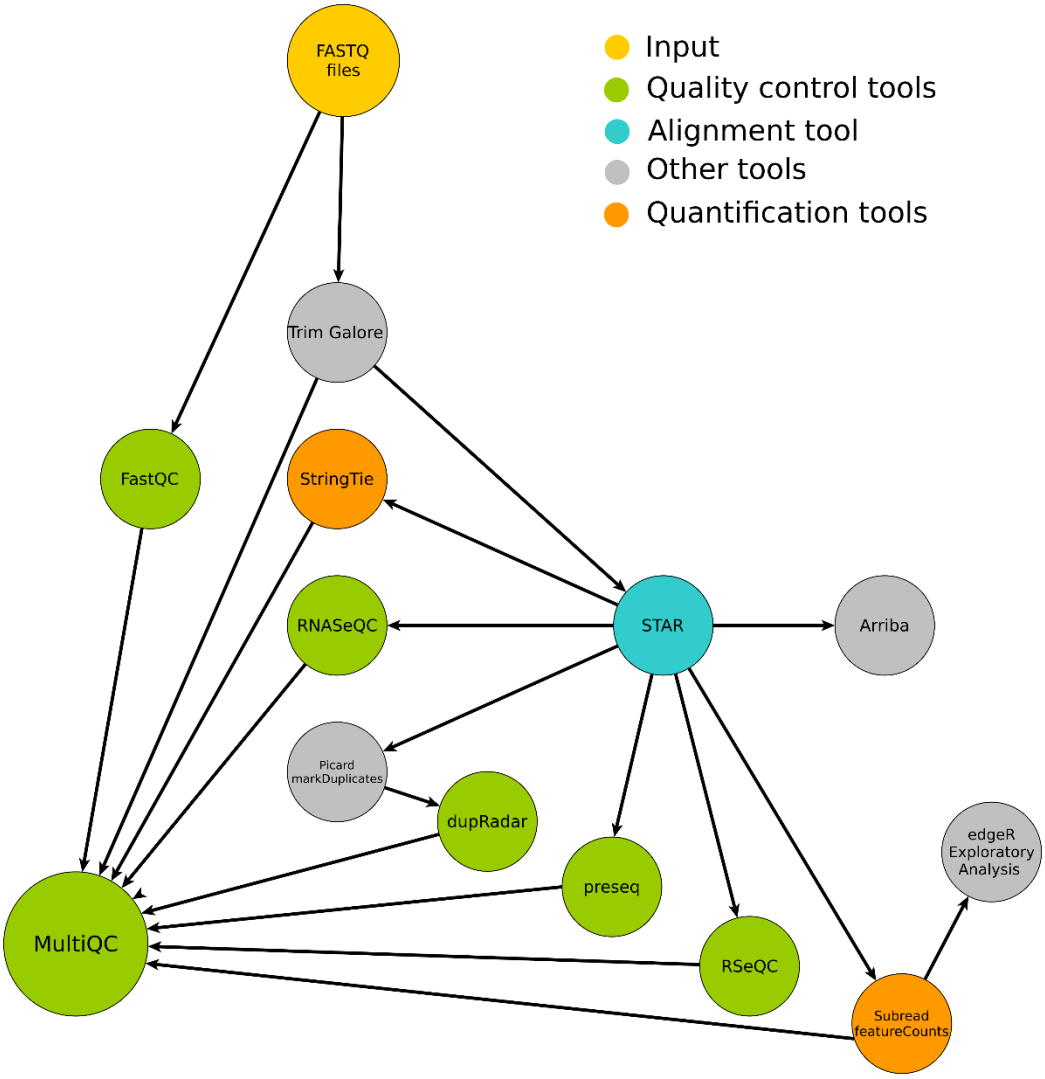

Figure 4. FIMM-RNAseq data analysis pipeline. FIMM-RNAseq incorporates quality control tools, such as FastQC and the pre-processing tool Trimgalore. It aligns RNASeq reads using a STAR[22] aligner and performs gene quantification and transcript assembly using Subread[23] and StringTie[24], respectively. Extensive RNASeq quality matrices are generated using RNASeQC[25], RseQC[26], dupRadar[27] and Preseq[28, 29]. An aggregated report from the major analysis steps is generated using MultiQC[30]. Exploratory data analysis is performed using R and edgeR[31]. As an optional component, the pipeline has the gene-fusion prediction tool Arriba[32].

Brain tissue sample collection for proteomic analysis

Guide tubes were transported from the operation room to the laboratory on ice immediately after removal from the brain, and the samples were prepared for cryopreservation within one hour, as described below. The instruments from different hemispheres of each patient were handled individually.

Guide tubes were rinsed from inside with 10 ml of ice-cold phosphate-buffered saline (Sigma-Aldrich) using a 27-gauge needle and syringe. The suspension was collected into a 15-ml conical tube on ice. The tissue was pelleted via centrifugation at +4°C with 400 x g for 15 minutes. After centrifugation, the supernatant was removed carefully, and the pellet was flash frozen in liquid nitrogen. The samples were stored at -70°C until analysis.

Sample preparation and LC-MS analysis

The cells were lysed, and the proteins denatured by adding 200 µL of 8 mol/L urea (Sigma-Aldrich), followed by 15 min sonication. Insoluble cell debris was removed via two rounds of centrifugation (15 min, 20817 G, 22 °C). Total protein content was measured with BCA assay (Thermo Scientific), the results of which are shown in Table S2.

Disulfide bonds were reduced with dithiothreitol (final concentration 5 mmol/L; Sigma-Aldrich), and the cysteine residues were carbamidomethylated with iodoacetamide (final concentration 15 mmol/L; Sigma-Aldrich), after which a pooled quality control (QC) sample was created by taking 31 µL of each sample and combining them. The proteins were digested with 2.5 µg of sequencing grade modified trypsin (Promega). The resulting peptides purified with C18 MicroSpin columns (The Nest Group, Inc.); for samples with > 60 µg of total protein, only 60 µg of total digested protein was taken for C18 purification, whereas for samples with < 60 µg of total protein, all of the sample was used. After C18 purification, the samples were evaporated to dryness with a vacuum centrifuge and stored at -20 °C.

Prior to LC-MS analysis, the samples were resolubilized with 15 min sonication in 30 µL of 1% acetonitrile + 0.1% trifluoroacetic acid in LC-MS grade water (all from VWR). The injection volume (between 2 and 10 µL) was determined based on the amount of total protein in the sample. The sample was injected into the LC-MS, separated with EASY-nLC 1000 (Thermo Scientific) using a 120 min linear gradient and detected with Orbitrap Elite MS (Thermo Scientific) using top20 data-dependent acquisition, in which the 20 most intense ions from each MS1 full scan are

fragmented and analyzed in MS2. Pooled QC samples were analyzed at the beginning and end of the run sequence, but they were removed from the final data analysis.

Protein identification and quantification were performed with Andromeda and MaxQuant[33,34] with the standard settings and using a reviewed *Homo sapiens* UniProtKB/Swiss-Prot proteome (20431 entries, downloaded on 2019-08-30; The Uniprot Consortium[35]). In addition, LFQ (label-free quantification) was enabled, and identification FDR < 0.01 filtering was applied on both the peptide and protein levels. The LFQ intensity was used as an estimate of protein abundance without further normalisation. From the output, we filtered decoy hits, proteins flagged as potential contaminants (but not serum albumin) and proteins identified with a modification site only. The LFQ intensities of all quantified proteins in all samples are presented in the Supplemental Data S2.

To account for the variable amounts of blood in the samples, the correlations of each protein's LFQ intensity with those of serum albumin and hemoglobin subunit alpha were calculated, but no filtering based on these correlations was applied. The correlations are listed in the Supplemental Data S2.

Bioinformatics

To compare the overlap between the published datasets, the g:Convert tool of the g:Profiler[36] web server was used to convert the identifiers to the same namespace (ENSG_ID).

Allen Brain Atlas Adult Human Brain Tissue Gene Expression Profiles[18] for the subthalamic nucleus and globus pallidus internal segment were downloaded from https://maayanlab.cloud/Harmonizome/dataset/Allen+Brain+Atlas+Adult+Human+Brain+Tissue+Gene+Expression+Profiles. The reference list was formed by including all the upregulated genes from both hemispheres of the anatomical structure to the same list.

The SynGO portal[19] was used to analyze the enriched terms in the RNAseq dataset. The used dataset was prepared for analysis by using the gene list that contained the overlapping genes among all RNAseq samples (n=9901). To make a list of the top 20% of expressed genes among this common gene set, the expression levels of individual genes were normalized against the total expression level of the sample. The average value of normalized expression levels was used to rank the genes according to their expression level from high to low, and top 20% (n=1980) identifiers were used for SynGO analysis. A list of the ranked genes and original SynGO results appear in Supplemental Data S3.

Gene ontology (GO) [37,38] enrichment analysis using DAVID[16,17] bioinformatics platform Version 6.8 was performed for the list of all identified proteins across all samples. The complete list of all enriched terms (FDR < 0.01) appears in Supplemental Data S2. Collapsed (DIR) GO terms are shown; the uncollapsed (ALL) GO terms are listed in Supplemental Data S2.

BioVenn[39] was used to draft area-proportional Venn diagrams. InteractiVenn was used to draw other Venn diagrams[40].

Author contributions

SK: study design, sample preparation protocols, sample collection, laboratory experiments, data analysis, and drafting the manuscript

JT: LC-MS experiments, method development and data analysis

ML: patient recruitment, sample collection, clinical data

AS: RNAseq method development

BG: RNAseq data analysis

PM: RNAseq experiment design

JU (shared last): study design, research ethics, supervision and funding

MV (shared last): study design, supervision and funding, method development, resources for LC-MS analysis

JK (shared last): study design, sample collection and funding

RH (shared last): study design, sample preparation protocols, sample collection, laboratory experiments, drafting the manuscript, supervision and funding

All authors discussed the results, read, and approved the final manuscript.

Funding

This work was supported by the Academy of Finland [Decision numbers #311934 R.H. (profiling programme) and #331436 J.U.], Pediatric Research Foundation, Finland (J.U. and R.H.), Biocenter Oulu (J.U. and R.H.), Biocenter Finland, Special State Grants for Health Research, Oulu University Hospital, Finland (J.U.) and the Terttu Foundation, Oulu University Hospital, Finland (J.K.).

Acknowledgements

Laboratory technician Pirjo Keränen is acknowledged for her assistance in sample collection. LC-MS analysis was performed at the Proteomics unit, University of Helsinki, and RNAseq experiments were performed by the Sequencing unit of Institute for Molecular Medicine Finland FIMM Technology Centre, University of Helsinki. Proteomics and Sequencing units are supported by Biocenter Finland.

Ethics declarations

Competing interests

The authors declare no competing interests.

References

1 Cilento, E. M. *et al.* Mass spectrometry: A platform for biomarker discovery and validation for Alzheimer's and Parkinson's diseases. *J. Neurochem.* (2019) doi:10.1111/jnc.14635.

2 Hosp, F. & Mann, M. A Primer on Concepts and Applications of Proteomics in Neuroscience. Neuron 96, 558–571 (2017).

3 Ping, L. *et al.* Global quantitative analysis of the human brain proteome in Alzheimer's and Parkinson's Disease. *Sci. Data* **5**, 180036 (2018).

4 McKetney, J. *et al.* Proteomic Atlas of the Human Brain in Alzheimer's Disease. *J. Proteome Res.* **18**, 1380–1391 (2019).

5 Li, K. W., Ganz, A. B. & Smit, A. B. Proteomics of neurodegenerative diseases: analysis of human post-mortem brain. *J. Neurochem.* (2018) doi:10.1111/jnc.14603.

6 Crecelius, A. *et al.* Assessing quantitative post-mortem changes in the gray matter of the human frontal cortex proteome by 2-D DIGE. *Proteomics* **8**, 1276–1291 (2008).

7 Zhu, Y., Wang, L., Yin, Y. & Yang, E. Systematic analysis of gene expression patterns associated with postmortem interval in human tissues. *Sci. Rep.* **7**, 1–12 (2017).

8 Sampaio-Silva, F., Magalhães, T., Carvalho, F., Dinis-Oliveira, R. J. & Silvestre, R. Profiling of RNA Degradation for Estimation of Post Morterm Interval. *PLoS One* **8**, e56507 (2013).

9 Dachet, F. et al. Selective time-dependent changes in activity and cell-specific gene expression in human postmortem brain. Sci. Rep. 11, 6078 (2021).

10 Buser, D. P. *et al.* Quantitative proteomics reveals reduction of endocytic machinery components in gliomas. *EBioMedicine* **46**, 32–41 (2019).

11 Ghantasala, S., Gollapalli, K., Epari, S., Moiyadi, A. & Srivastava, S. Glioma tumor proteomics: clinically useful protein biomarkers and future perspectives. *Expert Review of Proteomics* (2020) doi:10.1080/14789450.2020.1731310.

12 Abu Hamdeh, S. *et al.* Proteomic differences between focal and diffuse traumatic brain injury in human brain tissue. *Sci. Rep.* **8**, (2018).

13 Lozano, A. M. *et al.* Deep brain stimulation: current challenges and future directions. *Nat. Rev. Neurol.* **15**, 148–160 (2019).

14 Lahtinen, M. J. *et al.* A comparison of indirect and direct targeted STN DBS in the treatment of Parkinson's disease—surgical method and clinical outcome over 15-year timespan. *Acta Neurochir. (Wien).* **162**, 1067–1076 (2020).

15 Zaccaria, A. *et al.* Deep brain stimulation-associated brain tissue imprints: a new in vivo approach to biological research in human Parkinson's disease. *Mol. Neurodegener.* **11**, 12 (2016).

16 Huang, D. W., Sherman, B. T. & Lempicki, R. A. Bioinformatics enrichment tools: paths toward the comprehensive functional analysis of large gene lists. *Nucleic Acids Res.* **37**, 1–13 (2008).

17 Huang, D. W., Sherman, B. T. & Lempicki, R. A. Systematic and integrative analysis of large gene lists using DAVID bioinformatics resources. *Nat. Protoc.* **4**, 44–57 (2009).

18 Hawrylycz, M. J. et al. An anatomically comprehensive atlas of the adult human brain transcriptome. Nature 489, 391–399 (2012).

19 Koopmans, F. *et al.* SynGO: An Evidence-Based, Expert-Curated Knowledge Base for the Synapse. *Neuron* (2019) doi:10.1016/J.NEURON.2019.05.002.

20 Molinari, N. et al. Sample Pooling and Inflammation Linked to the False Selection of Biomarkers for Neurodegenerative Diseases in Top–Down Proteomics: A Pilot Study. Front. Mol. Neurosci. 11, 477 (2018).

21 Di Tommaso, P. et al. Nextflow enables reproducible computational workflows. Nat. Biotechnol. 35, 316–319 (2017).

22 Dobin, A. et al. STAR: ultrafast universal RNA-seq aligner. Bioinformatics 29, 15–21 (2013).

23 Liao, Y., Smyth, G. K. & Shi, W. The Subread aligner: fast, accurate and scalable read mapping by seed-and-vote. Nucleic Acids Res. 41, e108–e108 (2013).

24 Pertea, M. et al. StringTie enables improved reconstruction of a transcriptome from RNA-seq reads. Nat. Biotechnol. 33, 290–295 (2015).

25 DeLuca, D. S. et al. RNA-SeQC: RNA-seq metrics for quality control and process optimization. Bioinformatics 28, 1530–1532 (2012).

26 Wang, L., Wang, S. & Li, W. RSeQC: quality control of RNA-seq experiments. Bioinformatics 28, 2184–2185 (2012).

27 Sayols, S., Scherzinger, D. & Klein, H. dupRadar: a Bioconductor package for the assessment of PCR artifacts in RNA-Seq data. BMC Bioinformatics 17, 428 (2016).

28 Deng, C., Daley, T., Calabrese, P., Ren, J. & Smith, A. D. Estimating the number of species to attain sufficient representation in a random sample. arXiv (2018).

29 Deng, C., Daley, T. & Smith, A. D. Applications of species accumulation curves in large-scale biological data analysis. Quant. Biol. 3, 135–144 (2015).

30 Ewels, P., Magnusson, M., Lundin, S. & Käller, M. MultiQC: summarize analysis results for multiple tools and samples in a single report. Bioinformatics 32, 3047–3048 (2016).

31 Robinson, M. D., McCarthy, D. J. & Smyth, G. K. edgeR: a Bioconductor package for differential expression analysis of digital gene expression data. Bioinformatics 26, 139–140 (2010).

32 Uhrig, S. et al. Accurate and efficient detection of gene fusions from RNA sequencing data. Genome Res. (2021) doi:10.1101/gr.257246.119.

33 Cox, J. & Mann, M. MaxQuant enables high peptide identification rates, individualized p.p.b.-range mass accuracies and proteome-wide protein quantification. Nat. Biotechnol. 26, 1367–1372 (2008).

34 Cox, J. et al. Andromeda: A peptide search engine integrated into the MaxQuant environment. J. Proteome Res. 10, 1794–1805 (2011).

35 Consortium, T. U. UniProt: a worldwide hub of protein knowledge. Nucleic Acids Res. 47, D506–D515 (2018).

36 Raudvere, U. et al. g:Profiler: a web server for functional enrichment analysis and conversions of gene lists (2019 update). Nucleic Acids Res. 47, 191–198 (2019).

37 Ashburner, M. et al. Gene ontology: Tool for the unification of biology. Nature Genetics vol. 25 25–29 (2000).

38 The Gene Ontology Consortium. The Gene Ontology Resource: 20 years and still GOing strong. Nucleic Acids Res. 47, D330–D338 (2018).

39 Hulsen, T., de Vlieg, J. & Alkema, W. BioVenn - A web application for the comparison and visualization of biological lists using area-proportional Venn diagrams. BMC Genomics 9, 488 (2008).

40 Heberle, H., Meirelles, V. G., da Silva, F. R., Telles, G. P. & Minghim, R. InteractiVenn: A web-based tool for the analysis of sets through Venn diagrams. BMC Bioinformatics 16, 169 (2015).

Supplemental File S1

SDS-PAGE and Western blotting

First, we analyzed one pilot sample (not included in mass spectrometry sample series) to evaluate the protein content and size distribution using SDS-page and western blot (Figure S1). Stain-free gel imaging revealed that the samples contain proteins of a large size range. Western blotting detected neuron- and glia-derived proteins in the samples. Western blotting was used to identify proteins in the samples that are expressed by nervous tissue –specific cell types such as neurofilament L (neuronal marker), GFAP (astrocyte marker) and CNPase (oligodendrocyte marker).

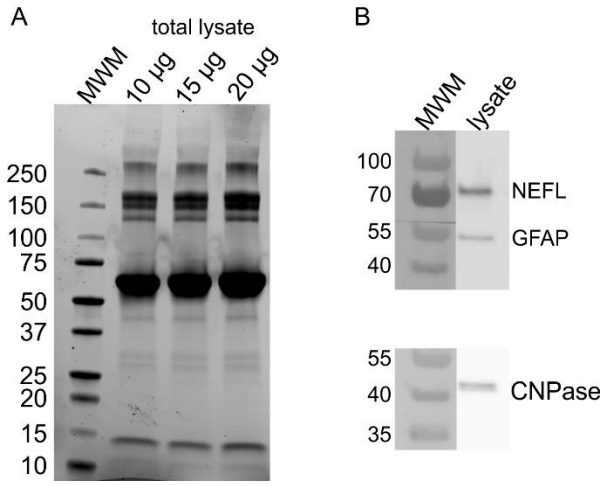

Figure S1. Image of SDS-PAGE gel and Western blot. A) 4-20% SDS-PAGE gradient gel (BioRad) was loaded with 10µg, 15 µg and 20µg of sample (total protein) and proteins were detected using stain-free ChemiDoc MP imaging system. B) Western blotting was used for identification of neurofilament L (neuronal marker, 1:1000), GFAP (astrocyte marker, 1:1000) and CNPase (oligodendrocyte marker, 1:1000).

Supplemental methods

Sample preparation for SDS-PAGE and Western blot

The frozen tissue pellet was thawed on ice and the proteins were solubilized as follows: 25 µl of protein solubilization solution (phosphate buffered saline containing 1,5 % n-Dodecyl β-D-maltoside (Sigma-Aldrich) and Protease Inhibitor cocktail (Pierce)) was added onto the pellet and mixed by vortexing. The samples were incubated on ice for 40-50 minutes and vortexed occasionally. After the incubation, the samples were centrifuged for 20 minutes at 20 000 x g at +4°C. The supernatant containing the solubilized proteins was transferred into a new microcentrifuge tube. The protein concentration of the sample was determined by using Bradford assay (Pierce). Solubilized protein samples were prepared for SDS-PAGE by adding Laemmli sample buffer (Biorad) containing 2-mercaptoethanol and incubating at room temperature overnight prior to running SDS-PAGE. To evaluate the protein content and size distribution in the sample, 4-20% Mini-PROTEAN® Stain-free TGX™ Precast Protein Gel (BioRad) was loaded with 10µg, 15 µg and 20µg of sample (total protein) and proteins were detected using stain-free ChemiDoc MP imaging system. For Western blotting, 20 µg of the protein sample was loaded into the 4–20% Mini-PROTEAN® TGX™ Precast Protein Gel (Biorad).

The gel was blotted onto nitrocellulose membrane (Trans-Blot® Turbo™ Mini Nitrocellulose Transfer Pack, BioRad) with Trans-Blot Turbo transfer system (Biorad). The primary antibodies to detect GFAP, CNPase and Neurofilament-L were from Neuronal Marker IF Antibody Sampler Kit (#8572, Cell Signaling Technology, MA, United States). The secondary antibody used was Goat anti-Rabbit IgG horseradish peroxide (HRP) (Abcam, Cambridge, UK), dilution 1:10000. The bands were visualized using WesternBright ECL Spray substrate (Advansta, CA, United States).